ChemComm

Distinguishing the Mechanism of Electrochemical Carboxylation in CO2 eXpanded Electrolytes

Journal:	*ChemComm*
Manuscript ID	CC-COM-12-2022-006560.R3
Article Type:	Communication

Journal Name

ARTICLE TYPE

Cite this: DOI: 00.0000/xxxxxxxxxx

Distinguishing the Mechanism of Electrochemical Carboxylation in CO_2 eXpanded Electrolytes

Matthew A. Stalcup,[a,b] Christian K. Nilles,[b,c] Bala Subramaniam,*[a,b] James D. Blakemore,*[b,c] and Kevin C. Leonard*[a,b]

Received Date
Accepted Date

DOI: 00.0000/xxxxxxxxxx

We shed light on the mechanism and rate-determining steps of the electrochemical carboxylation of acetophenone as a function of CO_2 concentration by using a robust finite element analysis model that incorporates each reaction step. Specifically, we show that the first electrochemical reduction of acetophenone is followed by the homogeneous chemical addition of CO_2. The electrochemical reduction of the acetophenone-CO_2 adduct is more facile than that of acetophenone, resulting in an Electrochemical-Chemical-Electrochemical (ECE) reaction pathway that appears as a single voltammetric wave. These modeling results provide new fundamental insights into the complex microenvironment in CO_2-rich media that produces an optimum electrochemical carboxylation rate as a function of CO_2 pressure.

Electrochemical CO_2 fixation is a grand challenge in sustainability science and is also significant in the context of the electrification of the chemical industry.[1] Specifically, selective synthesis of multicarbon products via electrochemical coupling of CO_2 remains challenging.[2] However, organic electrosynthesis has recently received increased attention due to its ability to precisely control reaction conditions and achieve novel reactivity patterns providing access to C-C bond formation.[3,4] Electrocarboxylation is a sub-class of organic electrosynthesis reactivity in which CO_2 is coupled to an organic backbone, enabling the formation of C-C bonds. In particular, electrocarboxylation of acetophenone produces atrolactic acid, a useful precursor for the production of nonsteroidal anti-inflammatory drugs (NSAIDs) such as ibuprofen and naproxen. This electrochemical route provides a greener alternative to the traditional production of hydroxyl carboxylic acids, which requires the use of cyanohydrins and the corresponding ketones.[5–12] However, achieving selective production of the carboxylic acid product remains difficult under most conditions due to competing alcohol production in protic solvents and reductive dimerization in aprotic solvents.[10,13–15] Additionally, the elementary steps involved in electrocarboxylation are not well understood, impeding further use of this reactivity mode to utilize waste CO_2 for the production of more useful chemicals.

In a prior report,[16] we demonstrated that CO_2-eXpanded Electrolytes (CXEs), electrochemical reaction media that support multi-molar CO_2 concentrations, enable the selective carboxylation of acetophenone (**1** in Figure 1) to produce atrolactic acid (**2** in Figure 1). We also observed that the selectivity of the reaction can be optimized by tuning the CO_2 concentration.[16] In the absence of CO_2 or at low (near atmospheric pressure) CO_2 concentrations, the rate of atrolactic acid production was low, and the reaction primarily produced 1-phenyl ethanol by net hydrogenation reactivity. At higher CO_2 concentrations, a dramatic increase in production of atrolactic acid occurred. Additionally, in our system, electrokinetic data collected as a function of CO_2 concentration revealed a surprising maximum rate of atrolactic acid production at 28 bar—the very highest CO_2 concentration resulted in diminished rates, despite the role of CO_2 as a substrate in the overall reactivity.

To gain insight into this counterintuitive CO_2 concentration dependence and shed light more broadly on the little-investigated mechanism of electrochemical carboxylation, we now report the development of a robust finite element analysis (FEA) model that incorporates the possible individual reaction steps and enables distinguishing the operative mechanism in CXE media. Others have modeled electrochemical CO_2 reduction systems, including the effects of electrode geometry, solution composition, and catalyst properties on kinetics and mass transport.[17–22] Our modeling work complements these studies by providing insight into the mechanistic pathway, overcoming the opacity of irreversible electrochemistry. The model takes into account transport and reaction in the 3D boundary layer adjacent to the electrode. Sev-

[a] Department of Chemical & Petroleum Engineering, University of Kansas, 4132 Learned Hall 1530 W 15th St, Lawrence, KS USA
[b] Center for Environmentally Beneficial Catalysis, University of Kansas, 1501 Wakarusa Drive LSRL Building A, Suite 110, Lawrence, KS
[c] Department of Chemistry, University of Kansas, 1140 Gray-Little Hall, 1567 Irving Hill Road, Lawrence, KS

† Electronic Supplementary Information (ESI) available: [details of any supplementary information available should be included here]. See DOI: 00.0000/00000000.

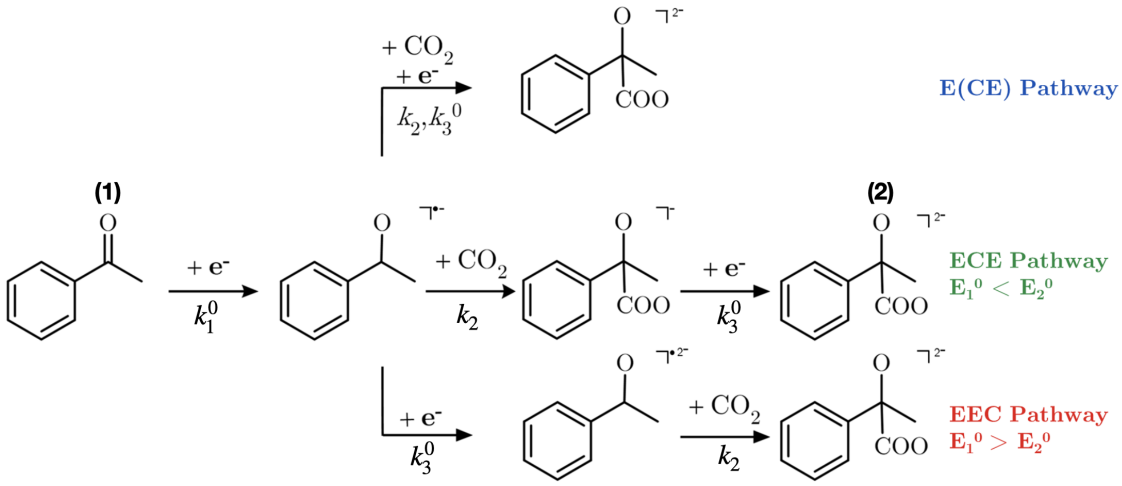

Fig. 1 Proposed reaction mechanisms for the electrochemical carboxylation of acetophenone for three different electrochemical reaction pathways. Electrochemical-Chemical-Electrochemical (ECE), Electrochemical-Electrochemical-Chemical (EEC), and Electrochemical-Concerted Chemical Electrochemical E(CE).

eral rival kinetic mechanisms were evaluated with the model to predict the experimental data acquired across varying scan rates and CO_2 concentrations. The kinetic mechanism that provided the best fit to the experimental data was deemed to be the most plausible.

In our mechanistic studies, we considered three possible schemes for the two-electron carboxylation reaction (Fig. 1): – (i) two electrochemical steps followed by a homogeneous chemical step (EEC), (ii) a homogeneous chemical step occurring between the electrochemical steps (ECE), (iii) and an electrochemical step followed by a concerted chemical-electrochemical step (E(EC)).[23] While several studies often treat the second electron transfer and carboxylation steps as a combined reaction step (E(EC)),[5,9,24] it was unclear at the outset of this work which of the three possible mechanisms best describes this optimum in rate versus CO_2 pressure.

We began the development of our FEA model by collecting cyclic voltammograms for the reduction/carboxylation of acetophenone at five different scan rates across five different CO_2 concentrations in CXEs. The electrochemical cell was a custom 50 mL Parr reactor modified for electrochemical use.[25] The electrolyte consisted of dry acetonitrile with dissolved tetrabutylammonium hexafluorophosphate ($TBAPF_6$) as the supporting electrolyte. A three-electrode system was used consisting of a glassy carbon working electrode (1 mm diameter), a Mg sacrificial counter electrode, and a glass-fritted silver reference electrode. The concentration of acetophenone remained constant at 0.1 M, accounting for the increase in volume as a function of pressure.[25,26] The reactor headspace pressure was varied from an argon atmosphere to CO_2 pressures ranging from 3.4 - 41.4 bar at 25°C. Under an argon atmosphere (Fig. 2, Ar sat), a single reduction wave was observed with no oxidation occurring on the reverse scan. The introduction of CO_2 (Fig. 2, 3.4 bar CO_2) results in a slight shift in the reduction wave in the less negative direction. Additionally, a significant increase in peak current is also observed.

Inspection of the voltammetry data shows that the carboxylation of acetophenone does not proceed via the EEC reaction pathway, as sequential reduction waves were not measured. In the absence of CO_2, the two-electron reduction of acetophenone and many other aromatic ketone molecules undergo sequential electron transfer with two distinct peaks in the voltammetry data.[8,24,27] This is typically believed to be attributable to the observation that the second electron transfer is more thermodynamically challenging than the first electron transfer. The absence of sequential electron transfer behavior in the voltammetry data thus speaks against the EEC reaction pathway in our system.

To probe the ECE reaction pathway, COMSOL Multiphysics was used to model the physicochemical processes underlying the carboxylation of acetophenone. The choice of the COMSOL software package over some more conventional voltammetry software packages was driven by its ability to simulate and visualize reactions and diffusion profiles in a 3-dimensional space (see Supporting Information Figure S12). The rate equations for the individual reactions (as given in Figure 1) were represented with individual elementary kinetic steps. Such an empirical kinetic modeling approach is necessary because it is very difficult, if not impossible, to experimentally measure the irreversible kinetics associated with this system. Without the presence of a return oxidation in the CV, it is not possible to determine parameters such as peak-to-peak separation that provide insights into the kinetics.

Details of the numerical model can be found in the Supporting Information. Briefly, the model relies on the actual experimental electrode geometry and calculates the predicted current accounting for the mass transfer properties of all species involved, the kinetics of both electron-transfer steps, and the kinetics of the homogeneous chemical step. The adjustable parameters which could be shifted to fit the simulation to the actual experimental cyclic voltammograms include the electrochemical rate constants (k_1^0 and k_3^0), the standard reduction potentials (E_1^0 and E_3^0), and

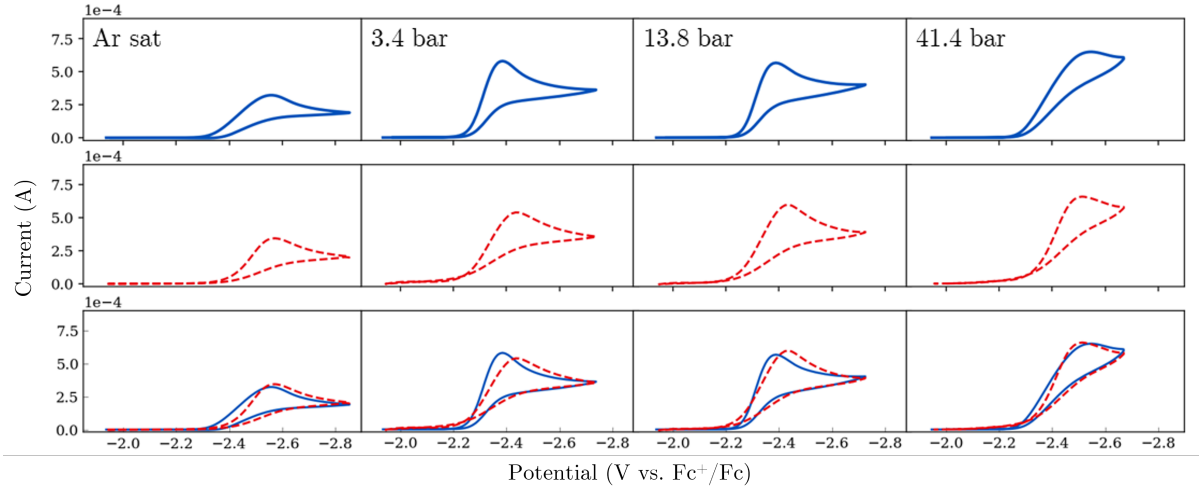

Fig. 2 Comparison of cyclic voltammetry of acetophenone carboxylation at 200 mVs^{-1} under argon saturated, 3.4 bar, 13.8 bar, and 41.4 bar CO_2 pressures on a 1 mm diameter glassy carbon electrode (solid line) with COMSOL simulations (dashed) where the potential is measured vs the Fc^+/Fc redox couple. The bottom row consists of overlayed experimental and simulated data.

the homogeneous reaction rate coefficient (k_2). The results of these simulations can be found in the center and bottom rows of Fig. 2. Supporting Information Table S1 shows the simulated kinetic information for the experiments at various CO_2 pressures.

We have found reasonable agreement between the COMSOL simulation results and the experimental voltammetric data at various CO_2 pressures. The correspondence of the simulated and experimental voltammograms at the various scan rates and at each pressure is shown in Figures S2-S6 in the Supporting Information. Under Ar-saturated conditions, the model predicted a single one-electron transfer voltammetric wave, as was observed experimentally (Figure S2). The absence of CO_2 made the reaction unable to proceed through the proposed ECE reaction pathway, and our simulation predicts this expected behavior.

At CO_2 pressures of 3.4 bar, 13.8 bar, and 28.6 bar, the model predicts an increase in the peak current and a slightly less negative shift in the onset, as was observed experimentally in each case. Examination of the simulated kinetic rate constants and standard reduction potentials for the electron transfer reactions show that the second reduction of the radical acetophenone-CO_2 adduct is more facile than the first reduction of acetophenone. This is a notable finding because the simulation shows that no direct CO_2 electrochemistry occurs during electrocarboxylation (i.e., no $CO_2^{\bullet-}$ radical is formed) and that the addition of CO_2 to the organic structure enables the second electron transfer. While a more detailed molecular dynamic model may be necessary to determine the involvement of concerted mechanisms, the second electron transfer can be reliably concluded to be significantly faster than the first. Additionally, the extracted kinetics for the homogeneous chemical step and the second electron-transfer step point to the ECE mechanism over the concerted mechanism. Both our simulations show a moderate lifetime for the acetophenone-CO_2 anion, and the size of a CO_2 molecule make a concerted mechanism less plausible.

As seen in the experimental data (Fig. 2, 41.4 bar CO_2), the voltammetric wave changes shape when the CO_2 pressure is increased to 41.4 bar. The simulation for the ECE mechanism fits the unique shape at this elevated pressure via decreasing the values of the kinetic rate constants for the electron transfer reactions while keeping their standard reduction potentials constant. Interestingly, we observed a similar pattern at higher CO_2 pressures during direct CO_2 electroreduction on a model polycrystalline gold catalyst in CXE media.[28] The COMSOL simulation predicted an attenuation of the electron transfer kinetic rate constant in this system as well. This suggests that the rate inhibition in the electrochemical reactions studied here and in our prior work[16,25,26] may be linked to a change in bulk property of the CXE medium (such as a lower polarity or conductivity) at higher CO_2 pressures that affect the mobility of available electrolyte ions and/or the structure of the electrochemical double layer.

Within the overall reaction paradigm described above, sensitivity analysis was performed by varying E_1^0, E_3^0, k_1^0, k_2, and k_3^0 to discern possible rate-determining step(s). The coefficient of determination, R^2, was used to infer the extent of sensitivity of the COMSOL simulation to various parameters, as shown in (Figures S7 – S11, Supporting Information). The parameters E_1^0 and k_1^0 were found to be most sensitive to changes in their values, suggesting that the first electron transfer is the rate-determining step.

As shown in Fig. 3a, the measured rate of production of atrolactic acid that was reported in our previous publication[16] shows a non-monotonic dependence on CO_2 headspace pressure (i.e., CO_2 concentration in the liquid phase). A plot of the product of k_1^0 and the liquid phase CO_2 concentration shows a similar trend (Fig. 3a, blue points). However, a plot of the regressed rate constant (k_1^0) vs. CO_2 head pressure (Fig. 3b) shows that while the rate constant remains virtually independent of CO_2 head pressure until 28 bar, it decreases rather steeply beyond this CO_2 pressure. Thus, a decrease in the rate of the first electron transfer dictates the behavior of our CXE-based system for electrocarboxylation, a reasonable conclusion since the analysis described above suggests

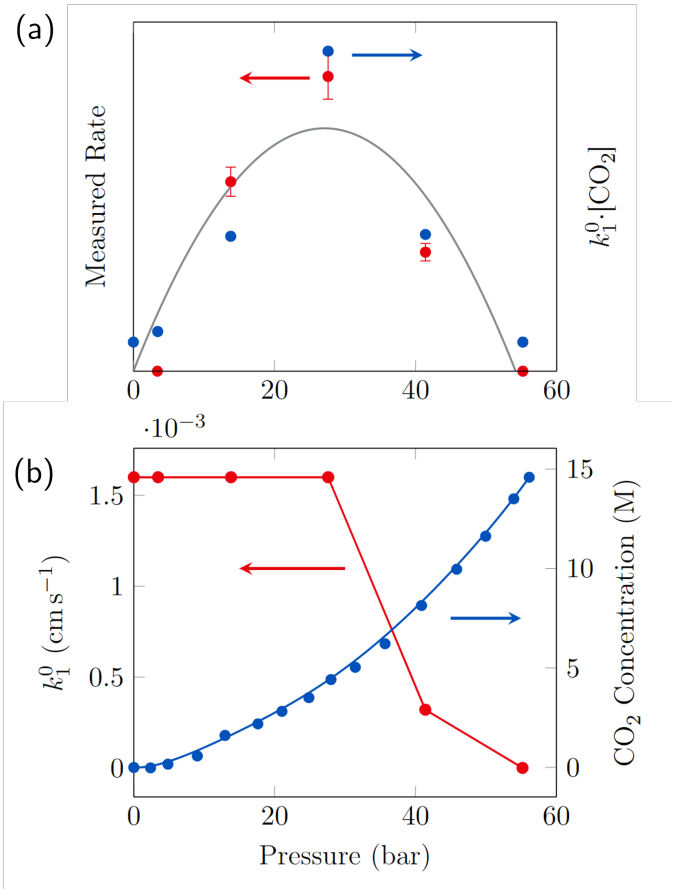

Fig. 3 (a) Comparison of the measured rate of atrolactic acid production from bulk electrolysis (red - from ref. 16) with the product of the simulated electron transfer kinetics and the CO_2 concentration (blue) at various CO_2 head-space pressures. (b) Simulated variation of electron-transfer kinetic rate constants (red) with CO_2 concentration in the CXE (blue) as a function of CO_2 head-space pressure.

that this step is rate determining. We attribute this drop to inhibition of ion transport in the CXE microenvironment, which could be dominated by non-polar CO_2 at the higher pressures of CO_2. Consequently, CO_2 can be viewed to inhibit the facile generation of acetophenone radicals at high CO_2 concentrations, resulting in an optimum CO_2 pressure that maximizes the rate of atrolactic acid formation by providing sufficient CO_2 to react while not using such high pressures that electron transfer is decelerated significantly through dissolution of very large quantities of CO_2.

In conclusion, the detailed modeling of the physicochemical processes underlying the electrochemical acetophenone carboxylation described here highlights the role of the CXE microenvironment at the electrode in governing reaction outcomes in CXEs. Our elucidation of a plausible rate determining step in the mechanistic model also helps unravel the origin of the non-monotonic dependence of rate on CO_2 pressure. These insights provide guidance for future interrogation of CXE microenvironments; these would have been inaccessible without global simulation of the voltammetry data to its irreversible nature. We emphasize that electrochemical carboxylation of acetophenone can occur in the CXE environment without direct CO_2 reduction, contributing to high rates and selectivities when sufficient liquid-phase CO_2 is present. These conditions thus avoid the need for production of $CO_2^{\bullet-}$, a species well known to be difficult to access under most conditions. On the other hand, the complexity of the microenvironment under ultra-high CO_2 concentrations (e.g., exceeding 5 M) results in a trade-off between CO_2 availability and enabling fast electron transfer. For the current system, this optimum pressure (ca. 30 bar) is fairly mild from an industrial and practical standpoint, making CXE media ideal for further development of practical electrocarboxylation systems.

Conflicts of interest

There are no conflicts to declare.

Acknowledgements

This work was funded by the U.S. National Science NRT program through Award No. DGE-1922649.

Notes and references

1 O. S. Bushuyev, P. De Luna, C. T. Dinh, L. Tao, G. Saur, J. van de Lagemaat, S. O. Kelley and E. H. Sargent, *Joule*, 2018, **2**, 825–832.
2 F. S. Roberts, K. P. Kuhl and A. Nilsson, *Angew. Chemie*, 2015, **127**, 5268–5271.
3 Y. Kawamata and P. S. Baran, *Joule*, 2020, **4**, 701–704.
4 X. Chang, Q. Zhang and C. Guo, *Angew. Chemie Int. Ed.*, 2020, **59**, 12612–12622.
5 A. A. Isse, A. Galia, C. Belfiore, G. Silvestri and A. Gennaro, *J. Electroanal. Chem.*, 2002, **526**, 41–52.
6 S. Wawzonek and A. Gundersen, *J. Electrochem. Soc.*, 1960, 537–540.
7 C. Amatore and A. Jutand, *J. Am. Chem. Soc.*, 1991, **113**, 2819–2825.
8 K. Zhang, H. Wang, S.-F. Zhao, D.-F. Niu and J.-X. Lu, *J. Electroanal. Chem.*, 2009, **630**, 35–41.
9 A. S. C. Chan, T. T. Huang, J. H. Wagenknecht and R. E. Miller, *J. Org. Chem*, 1995, **60**, 742–744.
10 S. F. Zhao, L. X. Wu, H. Wang, J. X. Lu, A. M. Bond and J. Zhang, *Green Chem.*, 2011, **13**, 3461–3468.
11 Q. Feng, K. Huang, S. Liu, J. Yu and F. Liu, *Electrochim. Acta*, 2011, **56**, 5137–5141.
12 S. F. Zhao, M. Horne, A. M. Bond and J. Zhang, *Phys. Chem. Chem. Phys.*, 2015, **17**, 19247–19254.
13 L. Zhang, L. P. Xiao, D. F. Niu, Y. W. Luo and J. X. Lu, *Chinese J. Chem.*, 2008, **26**, 35–38.
14 R. Matthessen, J. Fransaer, K. Binnemans and D. E. De Vos, *Beilstein J. Org. Chem.*, 2014, **10**, 2484–2500.
15 O. Scialdone, A. Galia, A. A. Isse, A. Gennaro, M. A. Sabatino, R. Leone and G. Filardo, *J. Electroanal. Chem.*, 2007, **609**, 8–16.
16 M. A. Stalcup, C. K. Nilles, H. J. Lee, B. Subramaniam, J. D. Blakemore and K. C. Leonard, *ACS Sustain. Chem. Eng.*, 2021, **9**, 10431–10436.
17 S. Suter and S. Haussener, *Energy & Environmental Science*, 2019, **12**, 1668–1678.
18 D. Bohra, J. H. Chaudhry, T. Burdyny, E. A. Pidko and W. A. Smith, *Energy & Environmental Science*, 2019, **12**, 3380–3389.
19 S. J. Cobb, V. M. Badiani, A. M. Dharani, A. Wagner, S. Zacarias, A. R. Oliveira, I. A. Pereira and E. Reisner, *Nature chemistry*, 2022, **14**, 417–424.
20 E. Edwardes Moore, S. J. Cobb, A. M. Coito, A. R. Oliveira, I. A. Pereira and E. Reisner, *Proceedings of the National Academy of Sciences*, 2022, **119**, e2114097119.
21 T. Burdyny, P. J. Graham, Y. Pang, C.-T. Dinh, M. Liu, E. H. Sargent and D. Sinton, *ACS Sustainable Chemistry & Engineering*, 2017, **5**, 4031–4040.
22 L.-C. Weng, A. T. Bell and A. Z. Weber, *Energy & Environmental Science*, 2020, **13**, 3592–3606.
23 A. J. Bard, Bard Allen J and L. R. Faulkner, *Electrochemical Methods : Fundamentals and Applications*, Wiley, New York, 2nd edn., 2001, p. 236.
24 B.-L. L. Chen, Y. Xiao, X.-M. M. Xu, H.-P. P. Yang, H. Wang and J.-X. X. Lu, *Electrochim. Acta*, 2013, **107**, 320–326.
25 C. I. Shaughnessy, D. J. Sconyers, T. A. Kerr, H. Lee, B. Subramaniam, K. C. Leonard and J. D. Blakemore, *ChemSusChem*, 2019, **12**, 3761–3768.
26 D. J. Sconyers, C. I. Shaughnessy, H. Lee, B. Subramaniam, K. C. Leonard and J. D. Blakemore, *ChemSusChem*, 2020, cssc.202000390.
27 S. F. Zhao, M. Horne, A. M. Bond and J. Zhang, *Green Chem.*, 2014, **16**, 2242–2251.
28 C. I. Shaughnessy, D. J. Sconyers, H.-J. Lee, B. Subramaniam, J. D. Blakemore, K. C. Leonard and E. Co, *Green Chem.*, 2020, **22**, 2434–2442.